Strong coupling through optical positioning of a quantum dot in a photonic crystal cavity

Susanna M. Thon,[1,a)] Matthew T. Rakher,[1,b)] Hyochul Kim,[1] Jan Gudat,[2] William T. M. Irvine,[1,c)] Pierre M. Petroff,[3,4] and Dirk Bouwmeester[1,2]
[1]*Department of Physics, University of California Santa Barbara, Santa Barbara, California 93106, USA*
[2]*Huygens Laboratory, Leiden University, P.O. Box 9504, 2300 RA Leiden, The Netherlands*
[3]*Department of Materials, University of California Santa Barbara, Santa Barbara, California 93106, USA*
[4]*Department of ECE, University of California Santa Barbara, Santa Barbara, California 93106, USA*

(Received 14 January 2009; accepted 2 March 2009; published online 20 March 2009)

Single self-assembled InAs quantum dots embedded in GaAs photonic crystal defect cavities are a promising system for cavity quantum electrodynamics experiments and quantum information schemes. Achieving controllable coupling in these small mode volume devices is challenging due to the random nucleation locations of individual quantum dots. We have developed an all optical scheme for locating the position of single dots with sub-10 nm accuracy. Using this method, we are able to deterministically reach the strong coupling regime with a spatial positioning success rate of approximately 70%. This flexible method should be applicable to other microcavity architectures and emitter systems. © *2009 American Institute of Physics*. [DOI: 10.1063/1.3103885]

Single quantum dots coupled to optical microcavities in the solid state are of interest for a variety of cavity quantum electrodynamics experiments. Potential applications include uses as quantum repeaters,[1] entangled photon sources,[2] and in measurement-based quantum computation schemes.[3,4] Photonic crystal defect cavities are of particular interest due to their small mode volumes, which enhance the electromagnetic field density and allow for the possibility of reaching the strong coupling regime. This advantage introduces an additional technological challenge which is that the quantum dot must be precisely located at the position of the antinode of the cavity field to achieve strong coupling, usually better than 60 nm in GaAs photonic crystals operating around 900 nm. This is made difficult by the random nucleation locations of the quantum dots in the semiconductor structure.

Past schemes for achieving strong coupling in photonic crystal cavities have relied largely on random chance[5,6] and often required the measurement of many devices before finding a cavity in which a quantum dot is both spectrally and spatially in resonance with the cavity mode. These devices have the additional complication that the photonic crystal cavity typically interacts with many emitters due to the large quantum dot density required to find a strongly coupled device. A deterministic coupling method based on using atomic force microscopy to locate the strain sites of buried quantum dots has previously been demonstrated.[7,8] Here, we present an all-optical method for measuring the positions of individual quantum dots that allows us to deterministically achieve strong coupling between a quantum dot and a photonic crystal cavity. This versatile method can be performed in the measurement setup at a very low quantum dot density and could be applied to many emitter-cavity systems. Our technique relies on the precise determination of the optical center of emission, similar to the biological technique of fluorescence imaging with one nanometer accuracy[9,10] that has been used to track the motion of molecular motors.

Our samples are grown by molecular beam epitaxy on a GaAs substrate. A ten layer $Al_{0.9}Ga_{0.1}As/GaAs$ distributed Bragg reflector is included under the 925 nm $Al_{0.7}Ga_{0.3}As$ sacrificial layer to enhance the intensity of the photoluminescence collected from the quantum dots. 65 nm of GaAs is grown on top of the sacrificial layer. Next, the InAs quantum dot layer is grown in the Stranski–Krastanov growth mode, and the partially covered island method[11] is used to blueshift the center of the quantum dot emission peak to approximately 920 nm. Finally, the sample is capped with another 65 nm layer of GaAs. After identifying a region on the wafer of suitable quantum dot density, an array of gold open-box markers are fabricated on the surface using electron beam lithography and a lift-off process. We work in a low quantum dot density regime of less than 1 μm^{-2} to ensure that there is only one quantum dot in our cavity volume with high probability.

Our positioning method relies on the fact that although the wavelength of our scanning laser is much larger than the required positioning accuracy, we can locate the center of the emission pattern very precisely by accurately fitting the emission peak and averaging over many scans. We are able to measure the center of the emission pattern to a statistical accuracy much better than the lateral size of the emitter without resolving its shape or size. The sample is mounted in a He-flow cryostat at 4.2 K, and a 780 nm diode laser is used to excite carriers above the bandgap of GaAs. We both excited and collected microphotoluminescence through a high power microscope objective which is mounted on an *XY* piezoelectric flexure stage with a scanning range of 100 μm. A dichroic beamsplitter directs the emission into a single mode fiber whose output is split and sent through two narrow-band interference filters and detected at two avalanche photodiodes (APDs). We identify individual quantum dots of interest located in suitable positions near the center of

[a)]Electronic mail: susanna@physics.ucsb.edu.
[b)]Present address: National Institute of Standards and Technology, Gaithersburg, Maryland 20899, USA.
[c)]Present address: Department of Physics, New York University, New York, New York 10012, USA.

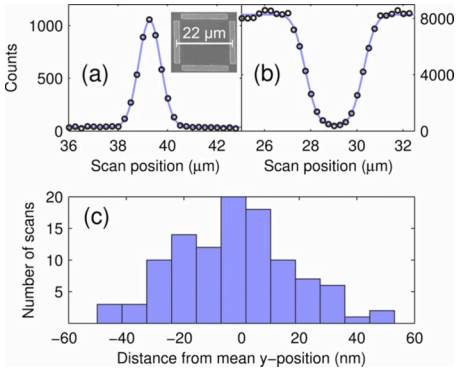

FIG. 1. (Color online) [(a) and (b)] Representative dot and wall scan data, respectively. The open circles are measured data and the blue lines are fits to the data. The inset shows a SEM image of the gold walls. (c) Histogram of the *y*-position of the quantum dot relative to one of the gold walls. This set of 106 scans yielded a statistical uncertainty in the dot *y*-position of 2 nm, given by $\sigma/\sqrt{N}$, where σ is the standard deviation of the Gaussian distribution, and N is the number of scans.

the gold boxes in our array and then use the piezoelectric stage to perform successive scans in the *X*- and *Y*-directions over the walls of the boxes and the quantum dot. Each scan passes over two walls, with the quantum dot signal in between. We monitor the signal near 920 nm on one APD and observe a peak at the location of the quantum dot. Simultaneously, on the other APD, we monitor the signal from the GaAs bandgap, near 820 nm, and observe a dip in signal at the locations of the box walls because the excitation laser is strongly reflected by the gold.

The individual quantum dot scans are fit to a Gaussian curve, and the wall scans are fit to a Gaussian convolved with a square function. Example fits to the data are shown in Figs. 1(a) and 1(b). In order to achieve high signal to noise ratios during the scans (about 30:1 for the quantum dot signal), it was critical to use a single mode fiber in the collection path. Enough successive scans are taken in the *X*- and *Y*-directions to build up sufficient statistics, and the measured relative positions of the quantum dot and the walls are roughly normally distributed as shown in Fig. 1(c). The error in the mean position of the quantum dot relative to the wall markers is $\sigma/\sqrt{N}$, where σ is the standard deviation of the Gaussian distribution of positions, and N is the number of scans. Thirty scans yields a statistical error of about 5 nm.

After the quantum dot positions are extracted, we fabricated photonic crystal cavities around the quantum dot locations using a standard electron beam lithography procedure.[12] The optimized *L*3-type design[13,14] that we used is shown in Fig. 2(a). The lattice parameters of each photonic crystal cavity are adjusted so that the resonant frequencies of

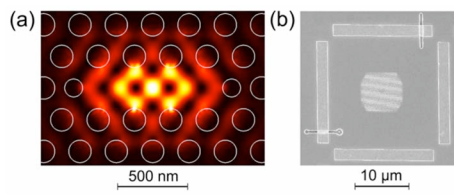

FIG. 2. (Color online) (a) Simulated electric field intensity in the modified *L*3-type cavity. The color scale goes from black (zero) to white (maximum intensity). (b) SEM image of a photonic crystal positioned near the center of a set of four gold markers. The lines on the upper and left markers are due to the detection procedure of the electron beam writer.

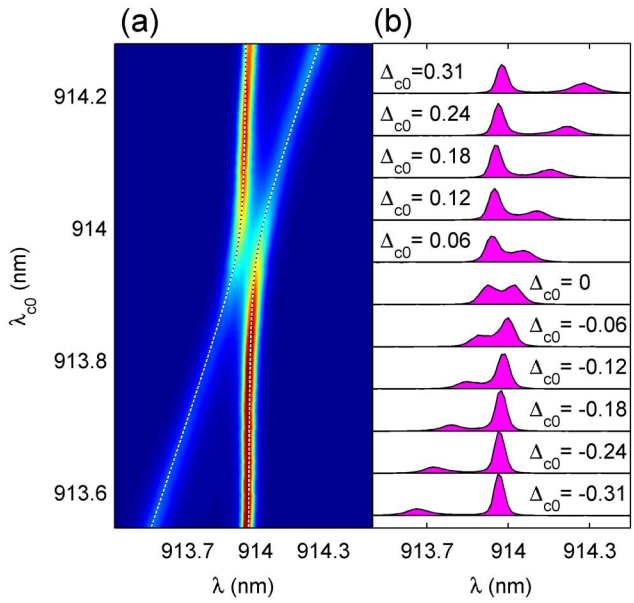

FIG. 3. (Color online) (a) Measured density plot of the spectra as the cavity mode is tuned into and out of resonance with the quantum dot exciton. λ_{c0} is the uncoupled mode wavelength. The dashed lines are the calculated peak positions which agree well with the measured positions. (b) Individual spectra at different values of Δ_{c0}, the uncoupled cavity mode detuning from resonance in nm.

the cavities are slightly blue of the quantum dot lines of interest. We aim to position the photonic crystal such that the quantum dot is at the central antinode of the electric field intensity, which has a width of about 120 nm. Using the direct write mode of the electron beam writer, we are able to detect the gold marks and write the photonic crystal pattern in the electron beam resist at the desired position to better than 30 nm accuracy as confirmed by scanning electron microscopy (SEM). The pattern is transferred into the device layer using Cl_2 based reactive ion etching, and the sacrificial layer is selectively etched with HF to create a membrane. Figure 2(b) is a SEM image of a fabricated photonic crystal device positioned relative to gold markers.

The same experimental setup that was used to measure the quantum dot positions is then used to measure the cavity properties. The only difference in the setup is that the emission is directed to a spectrometer equipped with a charge coupled device array instead of the APDs. We used the thin-film deposition method[15] to redshift the cavity toward the quantum dot line and observed the behavior on and near resonance. Due to variability during the electron beam write, about half of our cavity resonances are initially spectrally close enough to tune into resonance with the quantum dot; this percentage could be increased using digital etching.[16] We used an excitation power of about 250 nW to probe the system, such that our intracavity mean photon number is about 10^{-4} to ensure that we are in the vacuum Rabi regime. Of the devices in which we were able to tune through resonance, seven out of ten showed clear anticrossing behavior in the spectra, evidence of the strong coupling regime.

Figure 3(a) shows a measured density plot of the spectra as a function of the unperturbed cavity mode wavelength from one of our strongly coupled devices, together with the calculated peak positions. As the mode is redshifted toward the quantum dot wavelength, the two peaks repel each other, forming polariton states, and their linewidths become equal

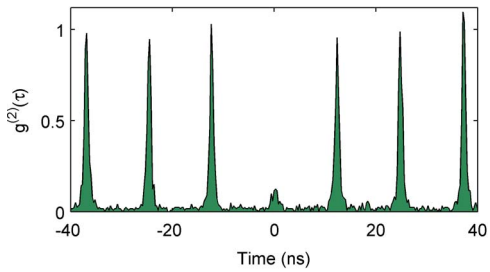

FIG. 4. (Color online) $g^{(2)}(\tau)$ measurement under pulsed excitation taken at the frequency of one of the polariton peaks. The peak at $\tau=0$ has an integrated area of $21\%\pm2\%$ the average area of the peaks at other times, demonstrating strong antibunching.

as seen in Fig. 3(b). The minimum energy separation ΔE is related to the Rabi frequency Ω and the linewidths of the cavity mode and exciton, γ_c and γ_x, respectively, by

$$\Delta E = 2\hbar\Omega = 2\hbar\sqrt{g^2 - \tfrac{1}{16}(\gamma_c - \gamma_x)^2}, \quad (1)$$

where g is the cavity-quantum dot coupling frequency. For the example device in Fig. 3, $\Delta E=132$ μeV, $\hbar\gamma_x=53$ μeV, and $\hbar\gamma_c=148$ μeV, corresponding to a Q factor of 9200 (typical devices had Q factors ranging between 8000 and 15 000). We note that the measured value for $\hbar\gamma_x$ is large compared to the true linewidth as the measurement is limited by the resolution of our spectrometer. From these values, we calculated $\hbar g=71\pm4$ μeV, which is about 55% of its maximum value determined from the cavity mode volume and transition dipole moment of the quantum dot.[17] The reduction in coupling constant can be attributed to a slight spatial offset of the quantum dot and cavity field maximum of less than 50 nm due to systematic errors in the positioning scheme and electron beam writer placement, combined with a small polarization mismatch of the exciton and cavity mode.[18] For our devices operating in the strong coupling regime, we calculated coupling constants between 31 and 78 μeV, with an average value of 63 μeV.

To confirm that in the strongly coupled devices the cavities were interacting with only one quantum dot, we measured the second order autocorrelation function, $g^{(2)}(\tau)$, of one of the polariton peaks when the cavity mode and exciton were tuned into resonance. The result for one such system, under pulsed excitation, is shown in Fig. 4. The area under the central peak at $\tau=0$ is $21\%\pm2\%$ of the average area of the peaks at other times, demonstrating that the photons emitted at the resonance frequency were strongly antibunched and that the cavity mode was interacting with only one exciton. Off-resonance, the photons collected at the mode frequency displayed decreasing evidence of antibunching.

In conclusion, seven out of ten of the devices in which we were able to reach spectral resonance displayed clear evidence of strong coupling, indicating that our positioning method is robust and deterministic. Precisely locating the positions of individual quantum dots is a necessary step toward realizing experiments involving networks of two or more quantum dots, such as generating entanglement between two quantum dots coupled to a single cavity mode.[19] Additionally, we note that this method is inherently flexible. A similar *in situ* optical lithography method applicable to relatively large cavity structures has been used to achieve weak coupling between quantum dots and micropillar cavity modes.[20] Because it does not require any special sample growth method, the optical positioning method could also be applied to many kinds of emitters, including *N-V* color centers in diamond, colloidal quantum dots, or fluorescent molecules in various microcavity architectures.

The authors would like to acknowledge G. Khoury, D. Kleckner, and B. Mitchell for useful discussions and experimental support. This work was supported by NSF NIRT Grant No. 0304678 and Marie Curie EXT-CT-2006-042580. A portion of this work was done in the UCSB nanofabrication facility, part of the NSF funded NNIN network. S.T. acknowledges financial support from the U.S. Department of Education GAANN grant.

[1] L. Childress, J. M. Taylor, A. S. Sörensen, and M. D. Lukin, Phys. Rev. Lett. **96**, 070504 (2006).
[2] C. Simon and J.-P. Poizat, Phys. Rev. Lett. **94**, 030502 (2005).
[3] E. Knill, R. Laflamme, and G. Milburn, Nature (London) **409**, 46 (2001).
[4] S. D. Barrett and P. Kok, Phys. Rev. A **71**, 060310 (2005).
[5] T. Yoshie, A. Scherer, J. Hendrickson, G. Khitrova, H. M. Gibbs, G. Rupper, C. Ell, O. B. Shchekin, and D. G. Deppe, Nature (London) **432**, 200 (2004).
[6] D. Englund, A. Faraon, I. Fushman, N. Stoltz, P. Petroff, and J. Vučković, Nature (London) **450**, 857 (2007).
[7] K. Hennessy, A. Badolato, M. Winger, D. Gerace, M. Atatüre, S. Gulde, S. Fält, E. L. Hu, and A. Imamoğlu, Nature (London) **445**, 896 (2007).
[8] M. Winger, A. Badolato, K. J. Hennessy, E. L. Hu, and A. Imamoglu, Phys. Rev. Lett. **101**, 226808 (2008).
[9] A. Yildiz, J. N. Forkey, S. A. McKinney, T. Ha, Y. E. Goldman, and P. R. Selvin, Science **300**, 2061 (2003).
[10] A. Yildiz, M. Tomishige, R. D. Vale, and P. R. Selvin, Science **303**, 676 (2004).
[11] P. M. Petroff, A. Lorke, and A. Imamoglu, Phys. Today **54**(5), 46, (2001).
[12] A. Badolato, K. Hennessy, M. Atatüre, J. Dreiser, E. Hu, P. M. Petroff, and A. Imamoğlu, Science **308**, 1158 (2005).
[13] Y. Akahane, T. Asano, B.-S. Song, and S. Noda, Nature (London) **425**, 944 (2003).
[14] Y. Akahane, T. Asano, B.-S. Song, and S. Noda, Opt. Express **13**, 1202 (2005).
[15] S. Strauf, M. T. Rakher, I. Carmeli, K. Hennessy, C. Meier, A. Badolato, M. J. A. Dedood, P. M. Petroff, E. L. Hu, E. G. Gwinn, and D. Bouwmeester, Appl. Phys. Lett. **88**, 043116 (2006).
[16] K. Hennessy, A. Badolato, A. Tamboli, P. M. Petroff, E. Hu, M. Atature, J. Dreiser, and A. Imamoglu, Appl. Phys. Lett. **87**, 021108 (2005).
[17] L. C. Andreani, G. Panzarini, and J.-M. Gérard, Phys. Rev. B **60**, 13276 (1999).
[18] K. Vahala, *Optical Microcavities* (World Scientific, Singapore, 2004), Chap. 4, p. 142.
[19] J. Metz, M. Trupke, and A. Beige, Phys. Rev. Lett. **97**, 040503 (2006).
[20] A. Dousse, L. Lanco, J. Suffczynski, E. Semenova, A. Miard, A. Lemaitre, I. Sagnes, C. Roblin, J. Bloch, and P. Senellart, Phys. Rev. Lett. **101**, 267404 (2008).